

## Application of Computed Global Radiation for Areas of High Relief

L. D. WILLIAMS,<sup>1</sup> R. G. BARRY<sup>2</sup> AND J. T. ANDREWS<sup>1</sup>

*Institute of Arctic and Alpine Research, University of Colorado, Boulder 80302*

(Manuscript received 26 July 1971, in revised form 13 December 1971)

### ABSTRACT

The variation over uneven terrain of the daily total of incident shortwave (global) radiation under cloudless conditions may be estimated by existing methods for calculating direct and diffuse solar radiation on a slope. A computer program for performing these calculations, incorporating a technique to determine when the direct rays of the sun are screened by the horizon at each point, is described. The adequacy of the approximation for diffuse radiation is considered by comparison with published data. Computations for an area of east Baffin Island, Northwest Territories, Canada, demonstrate that the occurrence of glaciers there is influenced both by elevation and by solar radiation. The potential of such computations as an aid in selecting station sites for climatological studies is also discussed.

### 1. Introduction

Solar radiation falling on slopes in mountainous terrain is of considerable significance in fields as diverse as forestry and glaciology. Few measurements are available although the effects of slope angle and orientation on clear sky radiation have been determined empirically (Turner, 1967; Hoinkes and Wendler, 1968; Kondratiev, 1969) and on theoretical grounds (Geiger, 1969), especially in middle latitudes. Most of the results have been presented in graphical or tabulated form (Lee, 1963; Bolsenga, 1964; Frank and Lee, 1966). Recently, Garnier and Ohmura (1968, 1970) discussed a computational method of calculating direct and global solar radiation income on slopes. We have made use of this approach in a study of the energy balance of glaciers and ice-free cirque basins in east Baffin Island, Northwest Territories, Canada. Most energy balance studies on glaciers are based on results from one or, at the most, two or three micrometeorological stations although the great complexity of spatial variations can rarely be treated satisfactorily on this basis. What is required is a control station, where actual receipts are measured, together with a computational means of extending the data over a larger area in a consistent and reliable manner. Goodison (1969) approached this problem for the Peyto Glacier, Alberta, by applying sunpath determinations (laboriously hand-calculated) for each point of interest on the glacier surface. By means of a computer, the method of Garnier and Ohmura can be used at each of a large number of points covering an area of interest to give a refined picture of the variability of solar radiation over

the area. Furthermore, a determination of the elevation of each point over a grid network (250 m spacing) allows an approximate determination of the times when each point will be shaded. For these times the computed direct component of radiation is omitted from the total. (Screening of the diffuse component has been omitted up to now. Its inclusion would considerably increase the computation time.) Ohmura (1968) mapped direct radiation on Mont St. Hilaire in this way and, in a later paper, Garnier and Ohmura (1970) included terms for shortwave diffuse and reflected radiation (the latter, however, was neglected because of its small contribution) to map global radiation on Barbados. Their method for determining screening by the horizon, however, was not specified, and it was assumed that data on the direct and diffuse radiation components were already available.

### 2. Computational procedures

Following Garnier and Ohmura (1968, 1970; Ohmura, 1968) the daily total of direct solar radiation falling upon a slope may be written

$$I_d = \frac{I_0}{r^2} \int p^m \cos(X \wedge S) dH, \quad (1a)$$

where  $I_0$  is the solar constant,  $r$  the radius vector of earth's orbit,  $p$  the mean azimuth-path transmissivity of the atmosphere,  $m$  the optical airmass,  $H$  the hour angle measured from solar noon, positive after noon, the integral being taken over the duration of sunlight on the slope, and  $\cos(X \wedge S)$  the cosine of angle of incidence of sun's rays on slope, equal to  $(-\sin\phi \cos H \cos A \sin\theta - \sin H \sin A \sin\theta + \cos\phi \cos H \cos\theta) \cos\delta + (\cos\phi \cos A \sin\theta + \sin\phi \cos\theta) \sin\delta$ . In this definition  $\phi$

<sup>1</sup> Also Department of Geological Sciences.

<sup>2</sup> Also Department of Geography.

is the latitude,  $A$  the slope of azimuth,  $\theta$  the slope angle, and  $\delta$  the declination of the sun.

As Garnier and Ohmura demonstrate, this expression is particularly useful for obtaining a reliable estimate of the variation of direct solar radiation over uneven topography when it is measured at only one point. This is done by obtaining a value for transmissivity by comparing measured with computed radiation and using this value to compute direct radiation at a set of grid points over the area in question. It was for such a purpose that the present authors adopted this approach; however, an independent programming effort was made to incorporate the following features: 1) an approximation to the clear-sky diffuse radiation, adding this to the direct radiation to obtain global radiation; 2) omission of the direct component from the daily total at times when a point is in the shadow of neighboring topography; 3) an expression for the optical airmass which is better than the secant approximation at low sun altitudes; and 4) production of radiation maps by computer-controlled microfilm plotter.

For computation, it is convenient to write (1a) in the form

$$I_d = \frac{I_0}{r^2} \int p^m (c_1 \sin H + c_2 \cos H + c_3) dH, \quad (1b)$$

where

$$\left. \begin{aligned} c_1 &= -\sin A \sin \theta \cos \delta \\ c_2 &= (\cos \phi \cos \theta - \sin \phi \cos A \sin \theta) \cos \delta \\ c_3 &= (\sin \phi \cos \theta + \cos \phi \cos A \sin \theta) \sin \delta \end{aligned} \right\}.$$

Alternatively, the quantity in parentheses in (1b) may be expressed as  $f(H) = c_4 \cos(H - \psi) + c_3$ , where  $c_4 = (c_1^2 + c_2^2)^{1/2}$  and  $\psi = \arctan(c_1/c_2)$ , i.e., as the equation of a cosine curve of amplitude  $c_4$  and phase angle  $\psi$  displaced from the  $H$  axis by an amount  $c_3$ . In the absence of shadow, the sun's rays are incident on the slope when this function is positive. The integral is evaluated at each grid point  $(i, j)$  by summation of positive values over small time intervals, i.e.,

$$I_{ij} = \frac{I_0}{r^2} \sum_{k=1}^n p^{mk} f_{ij}(H_k) \Delta H, \quad f_{ij}(H_k) > 0, \quad (2)$$

where  $n$  is the number of time intervals of length  $\Delta H$ . In agreement with Garnier and Ohmura, it is found that time intervals of 30 min give sufficient accuracy. The solar constant  $I_0$  is taken as  $2.0 \text{ cal cm}^{-2} \text{ min}^{-1}$ , and  $r$  is approximated as  $0.01676 \cos[\pi - 0.0172615(d - 3)] + 1$ , where  $d$  is the day of the year.

If diffuse radiation is measured at some point, or can be obtained as the difference between measured global and direct radiation, then it may be estimated at the grid points by means of the formula (Kondratiev, 1969)

$$D = D_0 \cos^2(\theta/2), \quad (3)$$

where  $D_0$  is the diffuse radiation on a horizontal surface

and  $\theta$  the slope angle. However, only the global radiation was measured in our glaciological field program on Baffin Island, as is the case in many instances. It is useful, therefore, to have a theoretical expression for diffuse radiation. This is an extremely complex problem (Kondratiev, 1969), and in our program we have used a simple clear-sky approximation given by List (1966, p. 420; attributed to Fritz) which estimates  $D_0$  from  $0.5[(1 - a_w - a_o)I_t - I_h]$ , where  $a_w$  is the proportion of radiation absorbed by water vapor (assumed to be 7%),  $a_o$  the proportion absorbed by ozone (assumed to be 2%),  $I_t$  the extraterrestrial radiation

$$(I_0/r^2) \int \cos z_s dH,$$

[ $z_s$  being the zenith angle of the sun],  $I_h$  the direct radiation on a horizontal plane at the surface

$$(I_0/r^2) \int p^m \cos z_s dH,$$

and the factor 0.5 expresses the assumption that half the radiation is scattered forward and half backward. Thus, using this formula in (3) we approximate diffuse radiation at each point  $(i, j)$  as

$$D_{ij} = \frac{I_0}{r^2} \sum_{k=1}^n (0.91 - p^{mk}) \cos z_s \Delta H \cos^2(\theta_{ij}/2). \quad (4)$$

Though simple, this expression appears to give reasonable results, at least for middle latitudes. Comparison of computed values was made with average measured values from Table 6.17 of Kondratiev (1969) for Pavlosk, Russia ( $59^\circ 41'N$ ), Benson, England ( $51^\circ 30'N$ ), Paris, France ( $48^\circ 49'N$ ), and Tacubaya, Mexico ( $19^\circ 24'N$ ). Fig. 1 shows the variation of computed diffuse radiation with transmissivity (in the range 0.5-0.9) for the 15th of each month for Pavlosk, compared with the average observational values. Measured values would coincide with theoretical values at transmissivities from 0.69-0.92. Table 1 gives the measured values and the transmissivities at which computed values would coincide with these. For Tacubaya some of the transmissivities required seem rather low, perhaps indicating that diffuse radiation is being underestimated by this method.

It must be emphasized that the only reason for incorporating this approximation for diffuse radiation into the present calculations is for comparison of calculated values with measured values of global radiation in order to arrive at a figure for transmissivity. Because of the anisotropy of clear-sky diffuse radiation, the intensity being greatest in the vicinity of the sun and near the horizon, its flux at the surface can be expected to vary with orientation of slope (Kondratiev, 1969). The formula, which assumes isotropic conditions, is

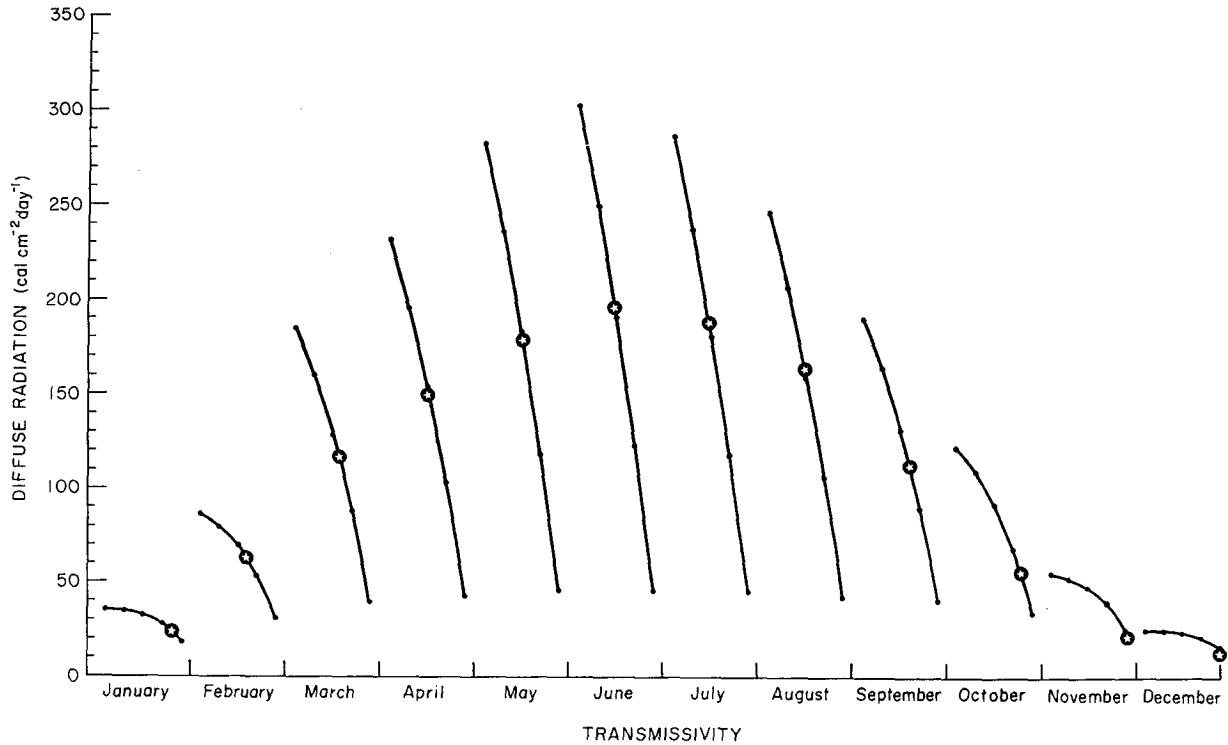


Fig. 1. Computed values of diffuse radiation ( $\text{cal cm}^{-2} \text{day}^{-1}$ ) at Pavlosk ( $59^{\circ}41'N$ ) for the 15th of each month for transmissivities in the range 0.5–0.9 (indicated by dots at 0.1 intervals, from left to right), compared to measured values (stars).

therefore of limited use for estimating the contribution of the diffuse component to spatial variations of global radiation. It is admirably suited, however, to obtaining

TABLE 1. Mean observed values of diffuse radiation ( $\text{cal cm}^{-2} \text{day}^{-1}$ ) and transmissivities at which computed values would coincide with them.

Location	Month					
	January	February	March	April	May	June
Pavlovsk	24 0.86	63 0.74	116 0.73	149 0.71	179 0.70	195 0.69
Benson	35 0.86	46 0.85	75 0.82	68 0.66	106 0.80	119 0.79
Paris	40 0.85	67 0.79	109 0.75	168 0.66	215 0.61	244 0.56
Tacubaya	88 0.71	82 0.73	186 0.50	252 ~0.3	268 ~0.3	201 0.50
Location	Month					
	July	August	September	October	November	December
Pavlovsk	188 0.69	164 0.69	113 0.75	55 0.84	22 0.91	13 0.92
Benson	128 0.76	119 0.76	106 0.76	103 0.71	45 0.84	24 0.91
Paris	234 0.56	191 0.61	135 0.69	85 0.77	48 0.84	35 0.86
Tacubaya	135 0.64	202 0.48	156 0.58	117 0.66	135 0.59	141 0.54

a value for transmissivity for, as Fig. 1 shows, over most of the year even a large error in the diffuse radiation estimate gives a small error in transmissivity. Moreover, although the magnitude of the spatial variation of clear-sky global radiation will be underestimated by neglecting anisotropy of the diffuse component, the spatial distribution of maximum and minimum values will not be affected since the flux of clear-sky diffuse radiation will vary with slope orientation in much the same way as the flux of direct solar radiation. It is the spatial variation of solar radiation which is of primary interest in east Baffin Island rather than the magnitude of its components.

Determination of whether a point is in shadow at any particular time is of critical importance in mountainous terrain and an algorithm for a solution to this problem was of major concern. No specific formulation of the problem has been noted in the literature. The determination is made by searching for an elevation along the line of the sun's azimuth great enough to obscure the sun. The elevations are obtained by interpolation of grid-point elevations  $E_{ij}$  at the intersections of the sun's azimuth with the grid lines. Thus, for the point  $(p, q)$ , if the sun's azimuth is at angle  $\alpha$  west of south ( $-\pi < \alpha < \pi$ ), the elevation at its intersection with the  $j$ th horizontal grid line is (with grid spacing  $\Delta x = \Delta y$ )

$$E'_j = (c \tan \alpha - a)E_{p-b,j} + (b - c \tan \alpha)E_{p-a,j}, \quad (5)$$

where  $c = q - j$ ,  $a = [c \tan \alpha]$ , the largest integer in  $c \tan \alpha$ ,

and  $b = a \pm 1$  (+ if  $\alpha > 0$ , - if  $\alpha < 0$ ); its intersection with the  $i$ th vertical grid line is at elevation

$$E_i'' = (f \cot \alpha - d)E_{i,q-e} + (e - f \cot \alpha)E_{i,q-d}, \quad (6)$$

where  $f = p - i$ ,  $d = [f \cot \alpha]$ , and  $e = d \pm 1$  (+ if  $|\alpha| < \pi/2$ , - if  $|\alpha| > \pi/2$ ). The distance from the point  $(p, q)$  to the point at  $E_j'$  is  $L_j' = |c \sec \alpha| \Delta y$ ; to the point at  $E_i''$  it is  $L_i'' = |f \csc \alpha| \Delta x$ . The point  $(p, q)$  will be in shadow when the sun's altitude is  $\Upsilon$  if, for any horizontal grid line  $j$ ,  $E_j' - E_{pq} > L_j' \tan \Upsilon$  or, if for any vertical grid line  $i$ ,  $E_i'' - E_{pq} > L_i'' \tan \Upsilon$ .

Of course, the array of elevations must ordinarily be larger than the array of radiation values in order to account for shading from outside the area of interest. The extent of outside topography to be considered must be arbitrarily determined by inspection of the topographic map, as this will vary with different areas. In order to reduce computation time, the program has been written to check for screening by the horizon only for a certain arbitrary distance unless the elevations  $E_j'$  and  $E_i''$  continue to increase. In the example discussed a distance of 1 km was found to be sufficient for each grid line.

As Garnier and Ohmura (1968, 1970) caution, and as can be seen from Table 3.1 of Robinson (1966), the secant approximation for the optical airmass,  $m = \sec z_s$ , is considerably in error for large zenith angles  $z_s$ . This being the case throughout much of the year in the arctic, we have used the optical airmass of a homogeneous spherical atmosphere (Robinson, 1966, p. 51) which agrees within 5% with Bemporad's values<sup>3</sup> for  $m$ . In fact, this proved to be an unnecessary refinement for the present study. Comparison of results using both approximations for the equinoxes at the arctic circle, conditions for which the discrepancy might be expected to be large, showed computed direct radiation at most 2% lower using the secant approximation (for all slopes, azimuths and transmissivities above 0.5). This arises because the major contribution to the daily total is around solar noon when the error in  $m$  is small. Even in the high arctic the improvement is only marginally significant; the same test run for 80N showed at most a 10% difference, more typically 5%, at the equinoxes and negligible difference at the summer solstice.

Where the range of elevations is large, a correction for reduction in airmass with elevation becomes fairly important (Robinson, 1966). This is usually derived by multiplying the airmass by the ratio of local pressure to normal sea level pressure. However, this quantity is not known at each point, so we approximate it, by integrating the hydrostatic equation for a homogeneous spherical atmosphere, as  $1 - (h/h_i)$  where  $h$  is local elevation and  $h_i$  the height of the atmosphere (taken as 10 km, by close agreement of airmass of homogeneous spherical atmosphere of that height with Bemporad's

values). For the present study, with an elevation range on the order of 1000 m, the pressure correction will be computed as 10% or about 100 mb. With the transmissivity  $p = 0.6$  and uncorrected  $m \approx 2$ , the correction to the factor  $p^m$  amounts to  $(p^{0.9m} - p^m)/p^m = (0.6)^{-0.2} - 1 = 0.108$ , or about 10%.

### 3. An example of application

The program described above was applied to a 7 km by 10 km area of east Baffin Island (67N, 63W) in order to determine the influence of solar radiation upon the presence or absence of cirque glaciers. The use of clear-sky radiation values is not a handicap since it is under such conditions that the spatial variation of incoming radiation, and therefore of snow and ice ablation, will be most pronounced. Fig. 2 shows the topography; the study area is outlined by the inner rectangle and the extent of present-day glaciers is indicated. From 9 June to 7 August 1970, global radiation was recorded continuously at a camp on the Boas Glacier by an actinograph and checked with a Moll-Gorczyński pyranometer. Comparison of recorded values with theoretical values for the four cloudless days during this period indicated transmissivities of 0.57, 0.65, 0.58 and 0.62. A value of  $p = 0.6$  was used in the program to compute radiation values on a  $29 \times 41$  grid over the area. Fig. 3 shows the variation in computed global radiation over the area for 21 June superimposed on a topographic map contoured from grid point elevations. Both sets of contour lines are traced from the microfilm output.

As expected, solar radiation is a significant factor in determining the location of glaciers in this area for they generally occur in places where clear-sky radiation is low ( $< 500 \text{ cal cm}^{-2} \text{ dy}^{-1}$ ). The correspondence is not perfect, however, and the effect of temperature decrease with elevation and possibly wind drifting of snow may influence the present distribution of ice bodies. Fig. 4 illustrates how the presence or absence of glaciers in existing cirques and valleys can be discriminated by the combined influence of global radiation and elevation. Each closed curve encompasses the value of global radiation and elevation of the grid points falling within a certain cirque or valley. While the radiation values are for 21 August, nearly identical charts but with higher radiation values were obtained for 21 June and 21 July. For the two largest glaciers, the upper and lower parts have been considered separately, the upper part roughly corresponding to the accumulation area where over the budget year net gain of snow and ice exceeds net loss, and the lower part roughly corresponding to the ablation area where loss of snow and ice exceeds gain but for addition of ice by glacier movement. It is seen that except for the two ablation areas there is a distinct break between the elevation-radiation regimes of the glacierized and non-glacierized cirques and valleys. The regimes of the latter, however, are overlapped by those

<sup>3</sup> See List (1966, p. 422).

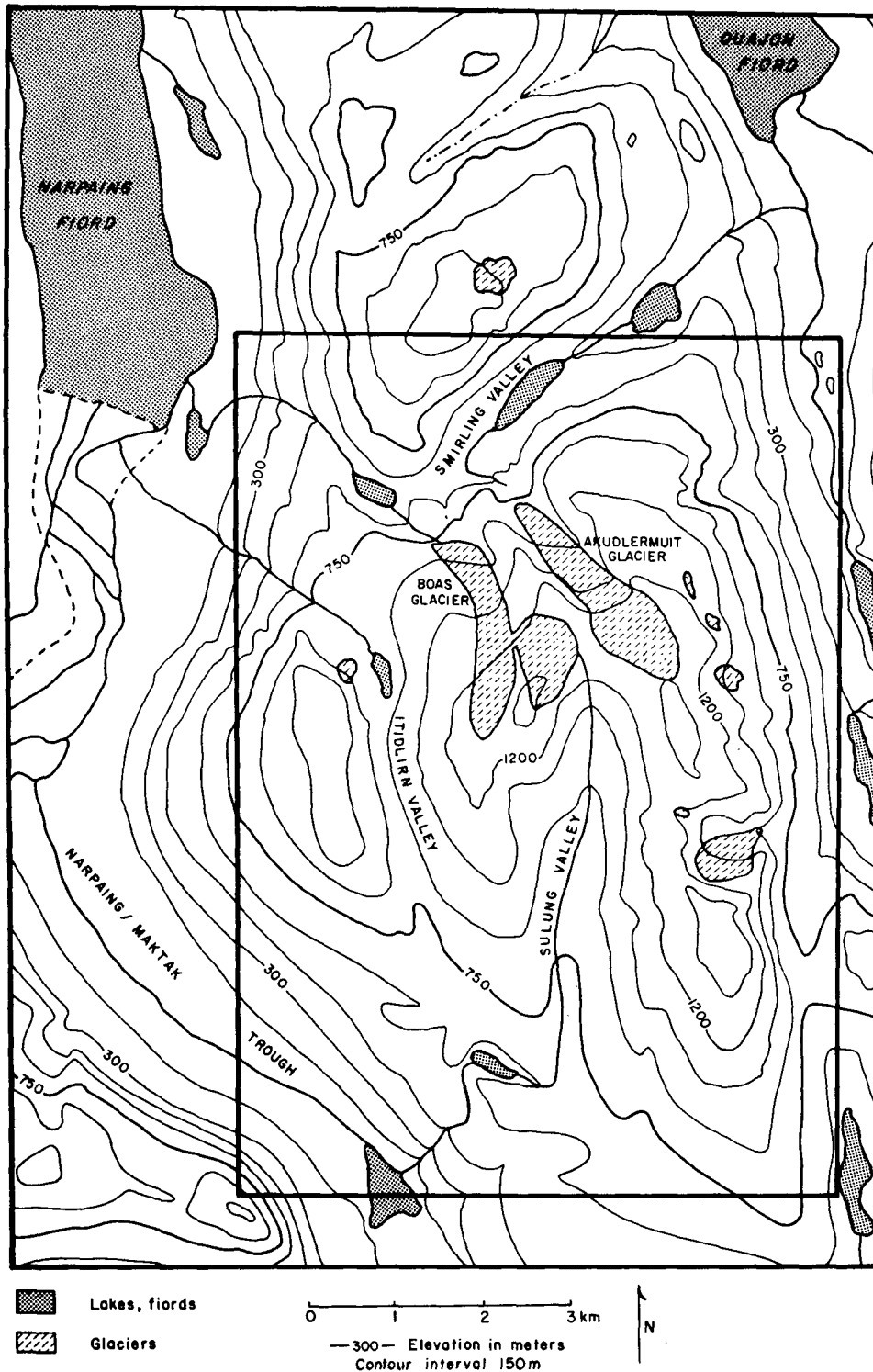


FIG. 2. Topography of the area between the heads of Quajon and Narpaing fiords, east Baffin Island, N.W.T., Canada. Area in rectangle is analyzed in Fig. 3.

of the ablation areas of the two larger glaciers, demonstrating the action of a valley glacier in moving ice down to an elevation at which it would not otherwise

persist. The particular effect of elevation on glacierization has not yet been investigated in detail. It may represent a combination of temperature decrease and

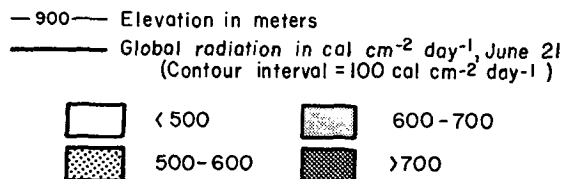
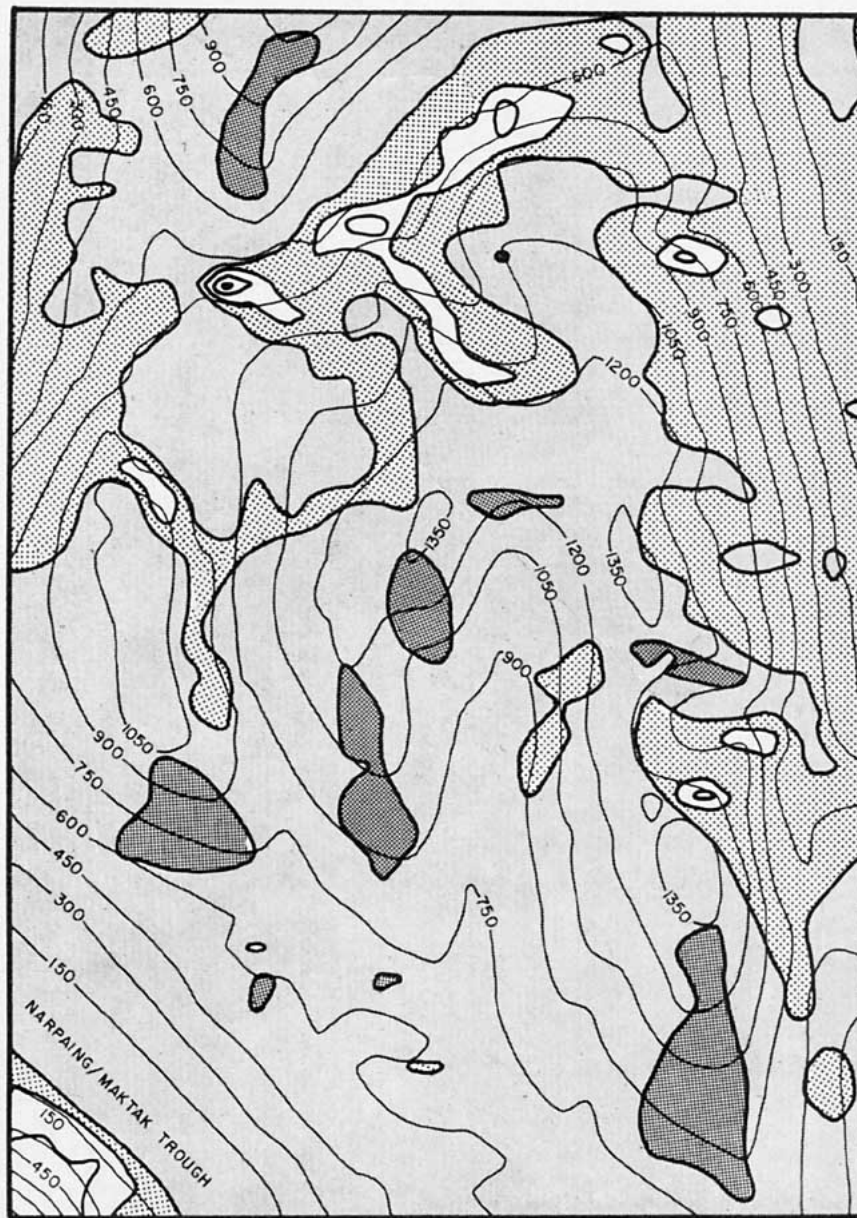


FIG. 3. Computed global radiation for 21 June under clear skies for the rectangular area in Fig. 2 superimposed on the topographic map of the area. Comparison should be made with Fig. 2 for the relationship of global radiation and distribution of ice bodies.

precipitation increase with height but factors such as wind drifting of snow cannot be neglected.

A graph like Fig. 4 may be useful in a number of ways. It can be used to delineate a theoretical local snowline based solely on clear-sky solar radiation values and

elevations. Comparison of graphs for different areas may reveal local climatic differences. For example, the overlap of glacierized and non-glacierized radiation-elevation regimes may point to the influence of wind drifting, avalanching, or some other factor.

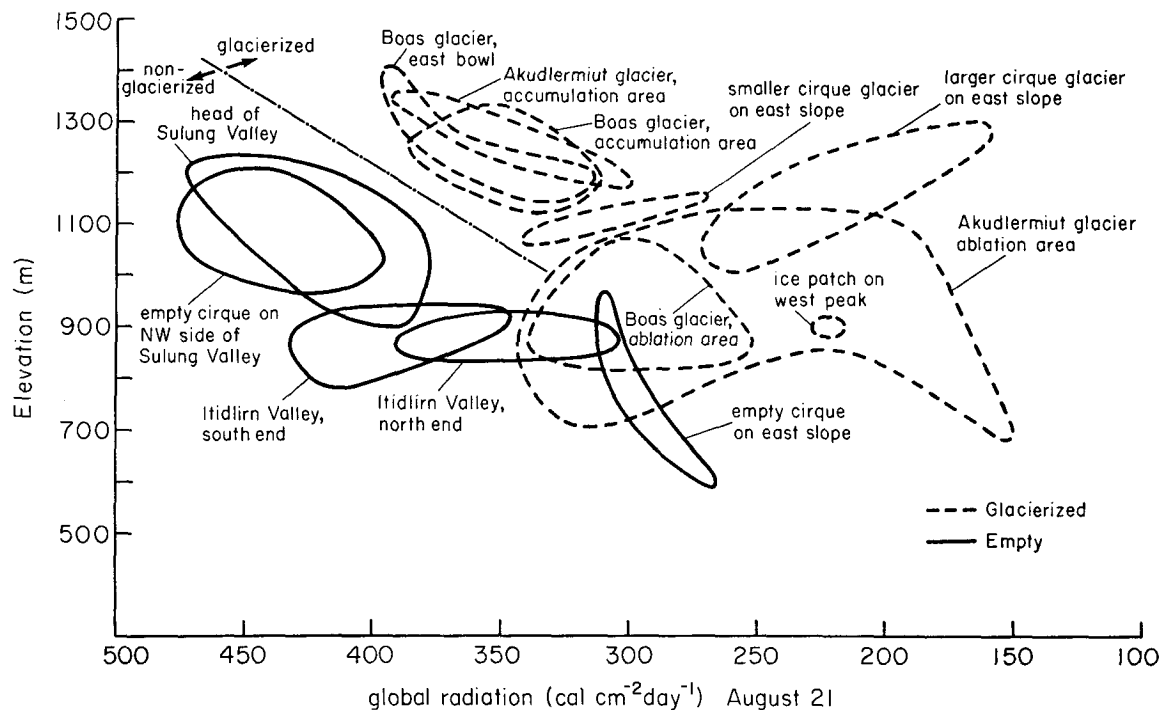


FIG. 4. Comparison of glacierized and non-glacierized valleys and cirque basins of Fig. 2 with respect to elevation and computed global radiation for 21 August. Each curve encloses the spread of values of elevation and global radiation for the individual basins.

Obviously maps of global radiation are still one step short of providing information on the spatial variation of net radiation which can account for 60–90% of the total energy contributing to ablation on glaciers in continental climatic regimes (Paterson, 1969). Point albedo values will modify the pattern of Fig. 4, but the inclusion of an albedo term will in general accentuate the “topography” of the radiation in Fig. 3, and in Fig. 4 the curves for the glacierized cirques will move further to the right, to lower radiation values, than will those for the non-glacierized cirques. Studies by J. D. Jacobs (personal communication, 1971) show that the average albedo during summer 1970 on the north-facing Boas Glacier, over snow, was 0.79. Albedos over the lichen-covered boulders in the surrounding terrain are probably around 0.15–0.20. An albedo value for each grid point could readily be included in the present program to provide a map of approximate absorbed solar radiation. The ratio of net radiation ( $R_n$ ) to absorbed solar radiation [ $S(1-\alpha)$ ] measured over 60 days on the glacier was 0.642. This figure could be used as representative of summers when little snow melt took place.

#### 4. Summary and further applications

An application of the computational procedure for determining direct, diffuse, and thus, global radiation on slopes of any angle and orientation in any latitude, incorporating the effects of horizon screening, has been described. Comparison of the calculated diffuse com-

ponent with measured values shows its formulation to be satisfactory for estimating transmissivity, although because clear-sky conditions are assumed and anisotropy is not considered, the absolute values of global radiation are subject to some inaccuracy.

Nevertheless, the ability to compute the important transmissivity coefficient from measured values of global radiation probably makes possible better estimates of clear-sky global radiation than could otherwise be obtained. The greater usefulness of this method, however, is in studying the variation of solar radiation incident upon uneven topography, for which its shortcomings are minimized by the following: 1) the greatest spatial variability will occur under clear-sky conditions since the direct component, which varies far more with slope angle and aspect than the diffuse component, will predominate; 2) the neglected anisotropy of the diffuse component would merely accentuate the spatial differences due to the direct component, diffuse radiation being greatest from the part of the sky nearest the sun; and 3) the influence of shading by nearby topography upon spatial variation of direct solar radiation is maximal under clear-sky conditions. Even some of the variation of diffuse radiation is allowed for by slope angle, the steeper slopes facing less of the sky.

In stating that the greatest variation is to be expected for clear skies, the assumption is that clear skies prevail throughout the day. If cloudiness occurs with equal frequency for different hours of the day, the model will indeed indicate extreme spatial variation, but where the

diurnal variation of cloudiness is pronounced this need not be true. For example, in the Front Range of Colorado the computations could be quite misleading as afternoon cloudiness is typical in summer and a west-facing slope will certainly receive less solar radiation than an east-facing slope of the same angle.

Our particular interest in developing this program was related to energy budget studies on mountain glaciers, but one potentially important application of such information in climatological research does not appear to have been noted previously. The maps of direct or global radiation on slopes in areas of complex terrain indicate the complete range of radiation climates that are experienced and their spatial extent. In siting weather stations in such areas for short-term measurement programs, it is usual to select sites on a subjective basis and on grounds of convenience. Prior preparation of a slope radiation map would, however, enable a rational basis to be adopted in that the most extreme sites, at least for radiation receipts, could be selected, or avoided, as the specific problem required. It would also ensure that a properly representative range of radiation conditions were studied and thereby provide a means of assessing the spatial representativeness of the measured conditions. In regions where a useful empirical relationship exists between global radiation and net radiation the output of the program could easily be modified to incorporate net radiation estimates. Such factors as the influence of clouds on global radiation are also feasible additions to the basic program. The chief application of these techniques will be to extend the results of the usually limited number (because of cost and manpower) of micrometeorological stations and thereby obtain a reliable estimate of received radiation and spatial variability over any large area.

For the 29×41 grid, the program used 24K storage and 90 sec central processor time on the CDC 6400.

*Acknowledgments.* The work was supported by the Army Research Office, Durham, N. C., under Grant DA-ARO-D-31-124-G1163 on "Present and Palaeoclimatic Influences on the Glacierization of Cumberland

Peninsula, Baffin Island." The subprogram used for contouring the results on microfilm was made available by David Robertson of the National Center for Atmospheric Research, Boulder, Colo.

The program deck described in the paper is available at cost on request from the authors.

#### REFERENCES

- Bolsenga, S. J., 1964: Daily sums of global radiation for cloudless skies. Res. Rept. 160, U. S. Army Cold Regions Research and Eng. Labs., 124 pp.
- Frank, E. C., and R. Lee, 1966: Potential solar beam irradiation on slopes: Tables for 30–50° latitude. Forest Survey Res. Paper, RM 18, U. S. Department of Agriculture, 116 pp.
- Garnier, B. J., and A. Ohmura, 1968: A method of calculating the direct shortwave radiation income of slopes. *J. Appl. Meteor.*, 7, 796–800.
- , and —, 1970: The evaluation of surface variations in solar radiation income. *Solar Energy*, 13, 21–34.
- GEIGER, R., 1969: Topoclimates. *General Climatology*, Vol. 2, *World Survey of Climatology*, Amsterdam, Elsevier Publ. Co., 105–117.
- Goodison, B., 1969: The distribution of global radiation over Peyto Glacier, Alberta. Part 1, Final Rept., to Geological Subdivision, Inland Water Branch, Ottawa, Canada, 46 pp.
- Hoinkes, H., and G. Wendler, 1968: Der Anteil der Strahlung an der Ablation von Hintereis—und Kesselwandferner (Ötztaler Alpen, Tirol) in Sommer 1958. *Arch. Meteor., Geophys. Bioklim.*, B16, 195–236.
- Kondratiev, K. Ya., 1969: *Radiation in the Atmosphere*. New York, Academic Press, 485–502.
- Lee, R., 1963: Evaluation of solar beam irradiation as a climatic parameter of mountain watersheds. *Colo. State Univ. Hydrol. Papers*, 2, 1–50.
- List, R. J., 1966: *Smithsonian Meteorological Tables*, 6th rev. ed. The Smithsonian Institution, Washington, D. C., 527 pp.
- Ohmura, A., 1968: The computation of direct insolation on a slope. *Climatological Bull. (McGill Univ.)*, No. 3, January 42–53.
- Paterson, W. S., 1969: *The Physics of Glaciers*. Oxford, Pergamon, 250 pp.
- Robinson, N., 1966: *Solar Radiation*. Amsterdam, Elsevier Publ. Co., 347 pp.
- Turner, H., 1967: Strahlungskartierung eines geliederten Gebirgshanges auf Grund von Messungen der räumlichen Komponenten der Globalstrahlung. *Proc. Ninth Intern. Tagung Alpine Meteorology, 1966*, Swiss Meteorological Institute, Zurich, 331–347.